Biol. Cell (2012) **104**, 452–461 DOI: 10.1111/boc.201100044

Research article

Dicer-1 is a key enzyme in the regulation of oogenesis in panoistic ovaries

Erica Donato Tanaka and Maria-Dolors Piulachs[1]

Institut de Biologia Evolutiva (Universitat Pompeu Fabra-Consejo Superior de Investigaciones Cientificas), 08003 Barcelona, Spain

Background information. In insects, the action of microRNAs (miRNAs) on oogenesis has been explored only in dipterans, which possess meroistic ovaries, a highly modified ovarian type. Here we study miRNA function in the most primitive, panoistic type of ovaries using the phylogenetically basal insect *Blattella germanica* (Dictyoptera, Blattellidae) as model.

Results. Dicer-1 (Dcr1), a key enzyme in miRNA biogenesis, was depleted using RNAi. Females treated with double-stranded RNA targeting Dicer-1, exhibited deep alterations in oocyte development; among them, the follicular epithelia of the basal oocytes did not develop, thus resulting in sterile females.

Conclusions. These effects derived from the absence of Dicer-1 suggest that miRNAs are crucial for the regulation of oogenesis in panoistic ovaries, the most primitive insect ovarian type.


Supporting Information available online

Introduction

The cockroach *Blattella germanica* is a hemimetabolous species with panoistic ovaries, the ancestral ovarian type in insects. In panoistic ovaries, all germinal cells differentiate and develop into oocytes, and the development of these oocytes takes place with the participation of follicular cells. These two cell types are responsible for the production of the mRNAs required to maintain oocyte development, as well as for maternal mRNAs, which are essential for embryo growth in the first few hours after the zygote formation. Although each *B. germanica* ovary has around 20 ovarioles, only a single oocyte per ovariole, the basal one, develops during a particular gonadotrophic cycle, whereas the development of subsequent oocytes is arrested until the onset of the next cycle. At 29°C, the first gonadotrophic cycle of *B. germanica* lasts for 8 days and comprises three characteristic phases encompassing the whole oogenesis process, namely previtellogenesis (from newly emerged adult, day 0, to day 2), vitellogenesis (from day 3 to 6) and choriogenesis (day 7) (Irles et al., 2009). In this cockroach, oogenesis is controlled by juvenile hormone (JH), and the growth and maturation of basal oocytes show a pattern similar to that of JH titres in the haemolymph (Treiblmayr et al., 2006). During the vitellogenic phase, JH and vitellogenin (Vg) show the highest rates of synthesis (Martin et al., 1998; Treiblmayr et al., 2006), and basal oocytes grow exponentially with the uptake of Vg, which reaches the oocyte membrane across the large intercellular spaces that are formed between follicular cells by contraction of the cellular volume, a phenomenon that has been termed 'patency' (Abu-Hakima and Davey, 1975). However, the basal oocytes of *B. germanica* start growing during the sixth nymphal instar (the last nymphal instar), when follicular cells increase in number and key mRNAs are produced or translated (Ciudad et al., 2006). Thus, when the sixth instar nymph moults to the adult stage, the basal oocytes are ready

[1]To whom correspondence should be addressed (email mdolors.piulachs@ibe.upf-csic.es).
Key words: *Blattella germanica*, Cockroach, *Drosophila*, Juvenile hormone, MicroRNA.
Abbreviations used: BgDcr1, *B. germanica* Dcr1; JH, juvenile hormone; miRNA, micro RNA; Vg, vitellogenin.

Figure 1 | Dicer-1 in *B. germanica* ovary

(**A**) Levels of BgDcr1 mRNA in sixth instar nymphs and adult ovaries of *B. germanica*, measured by qRT-PCR. Dotted line indicates the pattern of juvenile hormone (JH) titres in haemolymph (data from Treiblmayr et al., 2006). (**B**) Levels of BgDcr1 mRNA in ovaries after JH treatment. Newly emerged adult females were treated with 20 μg of JH III and dissected 24 h later. (**C**) Levels of BgDcr1 mRNA in ovaries of allatectomised females. The corpora allata were removed in newly emerged females and the ovaries were examined when females were 5 days old. All mRNA determinations data represent three biological replicates (mean $\pm$ SEM), and are indicated as copies of mRNA per 1,000 copies of U6.

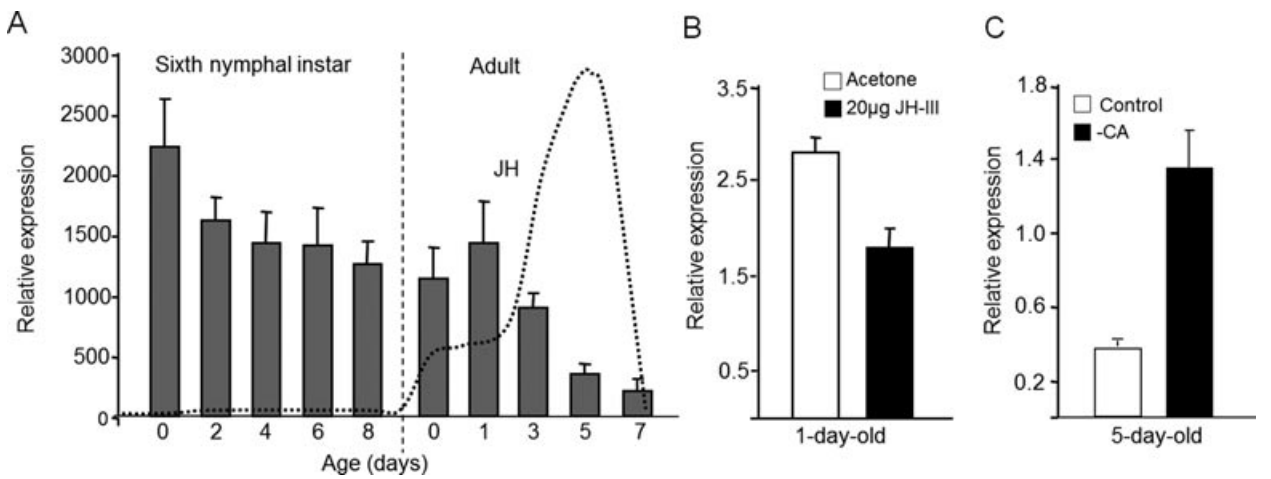

to grow, by uptaking the proteins (especially Vg) and lipids needed for embryo development (Ciudad et al., 2006, 2007).

Given that in panoistic ovaries no other cells support growth or provide materials to the maturing oocyte, the transcriptional and translational activity of the ovarian follicle must be finely controlled to modulate a precise dosage of regulatory proteins, thus avoiding meddling with zygote formation. MicroRNAs (miRNAs) appear to be essential to finely tune these processes by regulating gene expression or by removing undesired mRNAs at specific sites or times. However, and as discussed in recent reviews (Belles et al., 2012; Bushati and Cohen, 2007; Jaubert et al., 2007), information regarding the regulatory roles of these molecules is still fragmentary.

The discovery of small RNAs, including miRNAs, changed our view and understanding of the regulation of biological processes. As far as insects are concerned, miRNAs have been described and characterised in a number of holometabolous species whose genome sequence is known (Jagadeeswaran et al., 2010; Luo et al., 2008; Singh and Nagaraju, 2008; Skalsky et al., 2010; Stark et al., 2007; Weaver et al., 2007; Winter et al., 2007). Information regarding miRNAs in hemimetabolous species was initially only available for the migratory locust and the pea aphid (Legeai et al., 2010; Wei et al., 2009), but more recently, the miRNAs of *B. germanica* have been unveiled using high-throughput sequencing (Cristino et al., 2011).

B. germanica has two Dicer RNases, as occurs in other insect species (Belles et al., 2012). Dicer-1 (Dcr1), which is involved in transforming miRNA precursors into mature miRNAs (Gomez-Orte and Belles, 2009), and Dicer-2, which specialises on dicing double-stranded RNAs (dsRNAs) in the RNA interference (RNAi) pathway (unpublished results). A number of studies published in the last few years have involved manipulating the expression of Dicer as an approach to study the role of miRNA in insect oogenesis. This methodology has been followed in the fruitfly *Drosophila melanogaster* (Jin and Xie, 2007; Shcherbata et al., 2007) and the mosquito *Aedes aegypti* (Bryant et al., 2010), which are highly modified holometabolous species with meroistic ovaries. This approach has proven to be useful for describing the regulatory role of different miRNAs in insect oogenesis, from germline differentiation to axis formation in the egg chamber (Belles et al., 2012). Herein, we

Figure 2 | Expression of Dcr1 and miRNA in ovaries of dsBgDcr1-treated females

Females were treated with dsBgDcr1 or dsMock the day of emergence to adult. (**A**) Levels of BgDcr1 mRNA measured in 1-, 2-, 3- and 5-day-old treated females. (**B**) BgDcr1 protein in 0.1 ovary equivalents from 3- and 5-day-old treated females. (**C**) Expression levels of *B. germanica* miRNAs in 3- and 5-day-old treated females. In (**A**) and (**C**), the data shown are the values obtained in dsBgDcr1 knockdown animals normalised against the dsMock (reference value = 1). Asterisks indicate statistically significant differences when compared with respective controls ($P < 0.08$), according to analysis of variance test. All mRNA and miRNA determinations data represent three biological replicates.

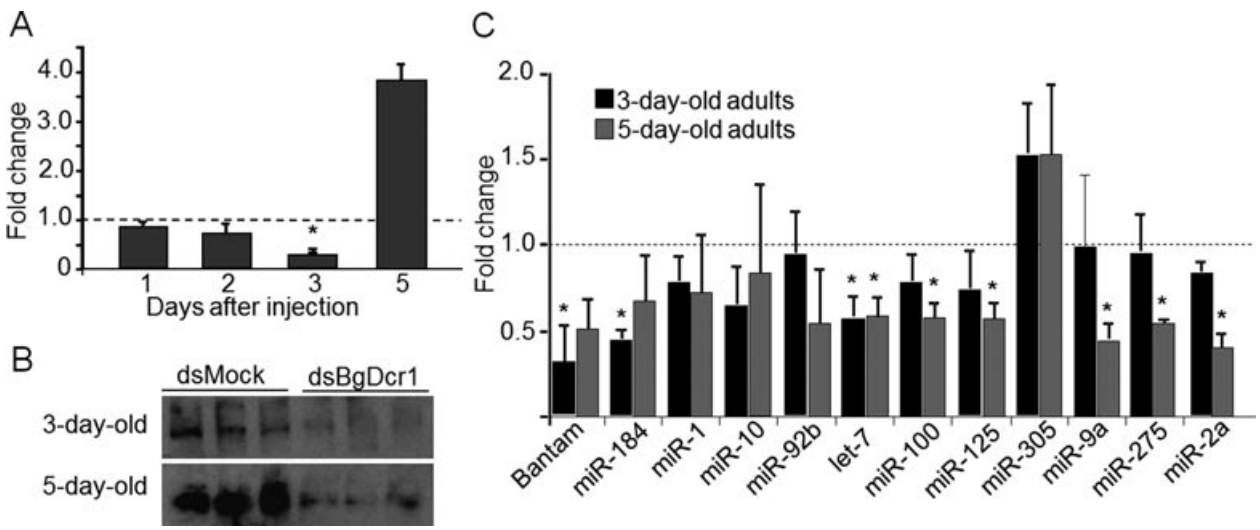

have used RNAi to knockdown Dcr1 in order to assess the importance of miRNAs in the regulation of oogenesis in a primitive hemimetabolous insect with panoistic ovaries.

Results

Expression of Dcr1 in the ovary

The expression pattern of *B. germanica* Dcr1 (BgDcr1) in the ovaries during the sixth nymphal instar, and in the adult during the first gonadotrophic cycle, was determined. The results (Figure 1A) showed that BgDcr1 has the highest expression levels at the onset of the sixth nymphal instar, subsequently decreasing as the basal oocyte matures, and reaching minimum values in the adult just prior to oviposition. Interestingly, BgDcr1 expression in the ovary follows a profile opposite to that of JH titres in the haemolymph (Figure 1A), thereby suggesting a possible cause–effect relationships.

In light of this, two different experiments were carried out to manipulate the JH levels in the haemolymph. In the first of these experiments, 20 μg of JH III was applied topically to newly emerged adult females, and BgDcr1 expression levels were measured 24 h later, at the moment of maximal expression in the gonadotrophic cycle. This JH treatment resulted in a significant decrease of BgDcr1 expression in the ovary (Figure 1B). The second experiment was performed by removing the corpora allata (CA), that is, the JH-producing glands, in newly emerged adult females, and measuring BgDcr1 expression levels 5 days later. The expression of BgDcr1 in these allatectomised females was 1,000-fold higher than in controls (Figure 1C).

Dcr1 knockdown affects miRNA expression and basal oocyte growth

We used RNAi to study the function of BgDcr1 and, by extension, the importance of the miRNAs in *B. germanica* oogenesis. Given that the oocyte starts growing during the sixth nymphal instar, and BgDcr1 levels during this period are higher than in the adult ovary, we carried out an initial set of experiments involving the injection of dsRNA targeting BgDcr1 (dsBgDcr1) into newly emerged sixth instar nymphs. After moulting to adult, the treated females were kept with males and left to oviposit. It was subsequently observed that control females (treated

with dsMock; $n = 20$) oviposited 8 days after adult emergence, whereas dsBgDcr1-treated females never oviposited ($n = 20$), while the basal oocytes had the same size as those of 6-day-old sixth nymphal instar (0.360 ± 0.01 mm; $n = 38$).

In another set of experiments, we treated newly emerged adult females with dsBgDcr1 ($n = 20$) or dsMock ($n = 18$) and they were observed daily. Although all dsMock-treated females oviposited 8 days after adult emergence, those treated with dsBgDcr1 did not oviposit and neither produced any trace of ootheca.

In a subsequent set of experiments, we treated newly emerged females with dsBgDcr1 ($n = 33$) or dsMock ($n = 33$); they were dissected 1, 2, 3 and 5 days after the treatment, and the expression levels of BgDcr1 in the ovaries was measured (Figure 2A). BgDcr1 levels 2 days post-treatment tended to be lower, and the decrease became clearer in ovaries from 3-day-old females, where the BgDcr1 expression level was almost 75% lower than in dsMock-treated females. However, mRNA levels in ovaries from 5-day-old-treated females showed an unexpected increase in BgDcr1 expression. The study of protein levels in 3-day-old-treated females revealed that BgDcr1 is practically absent from ovaries, while in 5-day-old females, BgDcr1 starts to become detectable (Figure 2B).

In order to examine whether changes in BgDcr1 expression affected miRNA levels in the ovary, a series of 12 miRNAs were chosen (taking in consideration their expression in ovaries; Supplementary Figure S1), and their levels measured in 3- and 5-day-old dsBgDcr1-treated females. In general, the miRNAs studied were down-regulated in both ages with respect to controls (Figure 2C). The decrease of bantam, miR-184 and miR-10 expression levels was stronger in 3-day-old than in 5-day-old females, as expected according to the corresponding decrease of BgDcr1, whereas the decrease of miR-1, miR-92b, miR-100, miR-125, miR-9a, miR-275 and miR-2a expression was more marked in 5-day-old dsBgDcr1-treated females. Let-7 expression decreased similarly in both ages. An interesting exception to this general tendency to down-regulation after dsBgDcr1 treatment was miR-305, which was found to be up-regulated in both 3-day-old- and 5-day-old-treated females.

Although the expression of BgDcr1 and most miRNAs was reduced after dsBgDcr1 treatment, oocyte growth in 3-day-old females did not appear to be affected (Figure 3A), as basal oocytes were found to have a similar length (0.70 ± 0.03 mm; $n = 11$) to those of dsMock-treated specimens (0.72 ± 0.04 mm; $n = 11$). Conversely, the basal oocytes in 5-day-old dsBgDcr1-treated females (0.50 ± 0.05 mm; $n = 13$) were smaller than in 5-day-old dsMock-treated females (1.47 ± 0.04 mm; $n = 13$), having a length which corresponds to 1-day-old non-treated adult female (Figures 3A, 3C and 3D).

Dcr1 knockdown affect follicular epithelium development

The morphology of basal oocytes of 5-day-old dsBgDcr1-treated females shows clear signs of size reduction, with the oocyte membrane commonly being folded and wrinkled (Figure 3E, arrowhead), thus making the stalk appear longer than usual. These features result from changes in the follicular cells that started when these females were 3 days old.

In 3-day-old *B. germanica* adult females, the follicular epithelium reaches the highest number of cells in the basal oocyte, at which point follicular cells begin to stop dividing, do not complete the cytokinesis and thus become binucleated (Figures 4A and 4D); 2 days later (5-day-old females; Figure 5A), all follicular cells are binucleated and no further divisions are observed. After dsBgDcr1 treatment, cell division was found to be frequent in 3-day-old oocytes (Figures 4E–4H), thus implying that the cells remained mononucleated (Figures 4E and 4H). Moreover, in dsMock-treated specimens actins located around the cell membrane, with higher concentrations being found at the cell junctions (Figure 4C), whereas they were not uniformly distributed around the cell membrane in dsBgDcr1-treated, but were observed invading the follicular cells cytoplasm, and showing very different levels of abundance between neighbouring cells (Figure 4G). These changes in the cytoskeleton are also reflected in the aspect of tubulins, with some cells that seem to lack these filaments after dsBgDcr1 treatment (Figures 4B and 4F), thus resulting in a notable disorganisation of the follicular epithelium.

The phenotype produced by dsBgDcr1 treatment is accentuated in 5-day-old females (Figure 5). At this age, ovarian follicles in dsMock-treated females exhibit patency at the epithelium, with large intercellular spaces between the binucleated cells

Figure 3 | Ovarian follicle development in dsBgDcr1 treated females

(**A** and **B**) Females were treated with dsBgDcr1 or dsMock at adult emergence and ovaries dissected 3 and 5 days later. (**A**) Length of basal oocyte (BOL, mm) ($n = 11$–13). (**B**) Diameter of follicular cells (μm) ($n = 40$–58). (**C**) Ovariole from a 5-day-old dsMock-treated female. (**D** and **E**) Ovariole from a 5-day-old dsBgDcr1-treated female. Asterisks indicate statistically significant differences when compared with respective controls ($P < 0.08$), according to analysis of variance test. The arrowhead indicates the shrinkage in the apical pole of basal oocyte. Immunofluorescence for β-tubulin (green), Phalloidin-TRITC staining for F-actin (red) and DAPI staining for nucleic acid (blue). Bo, basal oocyte; Sbo, sub-basal oocyte. Scale bars, (**D** and **E**) 100 μm, (**F**) 20 μm.

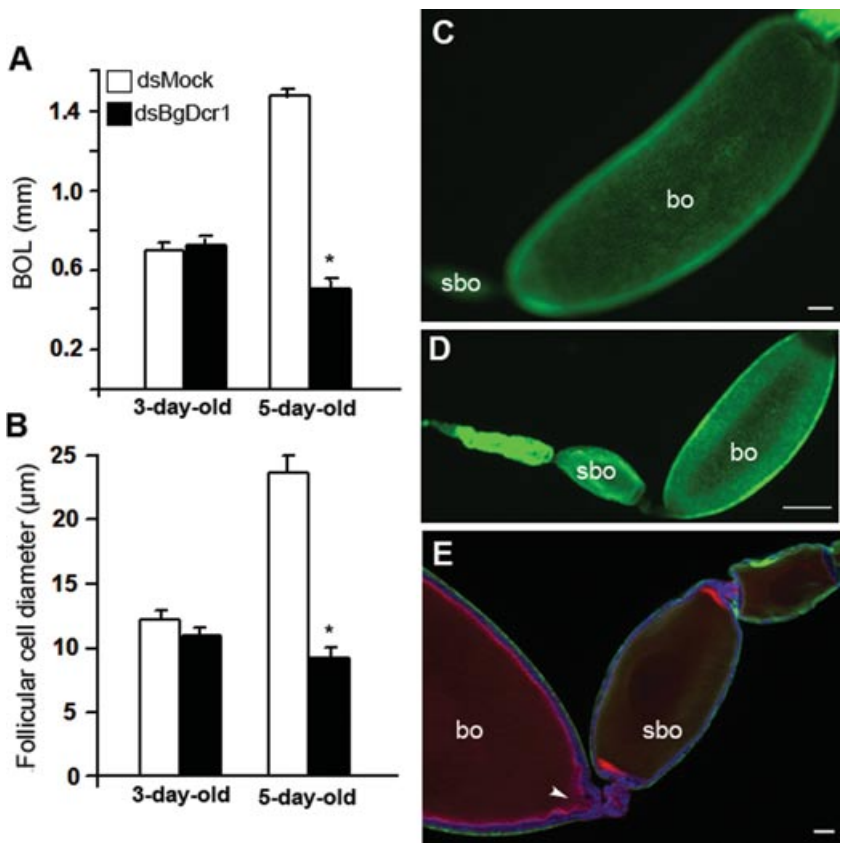

(Figure 5A). In contrast, the follicular cells in dsBgDcr1-treated specimens lost the current morphology (Figures 5B–5D), are smaller (Figure 3B) and appear to be affected in different ways, as follows. In a number of treated females, the follicular cells still undergo mitosis and a few of them are binucleated (Figure 5C), whereas others are mononucleated with and stretched aspect (Figure 5B) and show no signs of patency (Figures 5B–5D). The number of follicular cells in the basal oocytes of these females corresponds to that of a 5-day-old dsMock-treated female (9,000 cells/basal oocyte), whereas the basal oocytes show a size corresponding to a normal 1-day-old specimen (0.50 ± 0.05 mm).

Discussion

The development of basal oocytes in *B. germanica* starts in the sixth nymphal instar, when the follicular epithelium is proliferating and the oocyte shows extensive mRNA expression and translation (Ciudad et al., 2006). These findings suggest that a fine control of these processes should operate during this period of oocyte development, and that miRNAs might be good candidates to play a role in this fine-tuning. As Dcr1 is a key enzyme in the biosynthesis of the miRNAs (Belles et al., 2012), the high expression of BgDcr1 mRNA in *B. germanica* ovaries during the sixth nymphal instar and the first few days of adult life supports the above hypothesis. The

Figure 4 | Follicular epithelia in 3-day-old females treated with dsBgDcr1

Females were treated with dsMock (**A–D**) or dsBgDcr1 (**E–H**) at adult emergence and ovaries dissected 3 days later. Arrow in (**E**) indicates cells in division. Immunofluorescence for β-tubulin (green), Phalloidin-TRITC staining for F-actin (red) and DAPI staining for nucleic acid (blue). Scale bar, 10 μm.

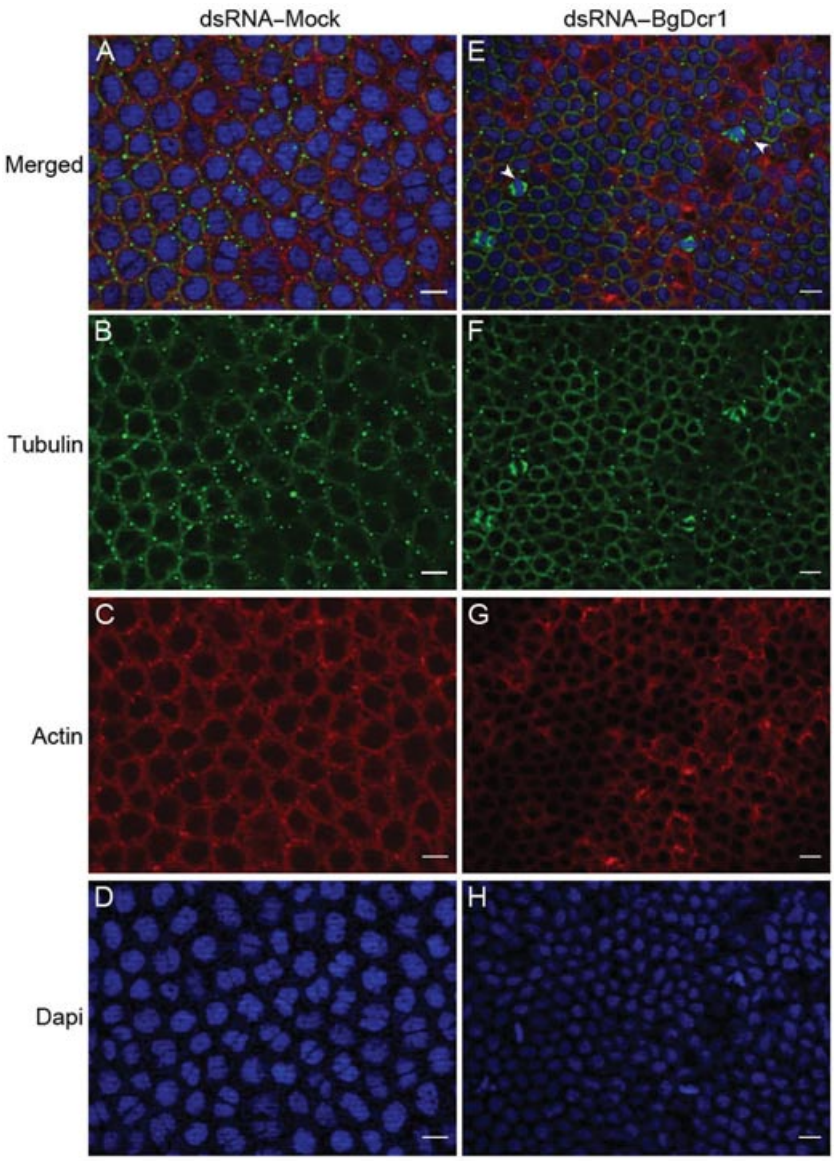

decrease of BgDcr1 expression observed in ovaries from 3-day-old adult females coincides with a change in the oocyte development program elicited by the increase of JH levels in the haemolymph (Treiblmayr et al., 2006). This hormonal signal determines that the fat body starts synthesising and releasing Vg, and that oocyte starts uptaking Vg from the haemolymph (Martin et al., 1998). In addition, it is also a key moment for the follicular cells that on day 3 cytokinesis stops and they become binucleated; moreover, as JH levels increase in the haemolymph, patency develops in the follicular epithelia. The fact that the decrease of BgDcr1 expression coincides with high levels of JH in the female haemolymph suggests that JH might inhibit BgDcr1 expression in the ovary. Indeed, our results are in agreement with this suggestion, as the

Figure 5 | Follicular epithelia from 5-day-old females treated with dsBgDcr1

Females were treated with dsBgDcr1 or dsMock at adult emergence and ovaries dissected 5 days later. (**A**) Follicular cells from dsMock. (**B–D**). Follicular cells from dsBgDcr1-treated females, showing different degree of affectation. Immunofluorescence for β-tubulin (green), Phalloidin-TRITC staining for F-actin (red) and DAPI staining for nucleic acid (blue). Scale bar, 10 μm.

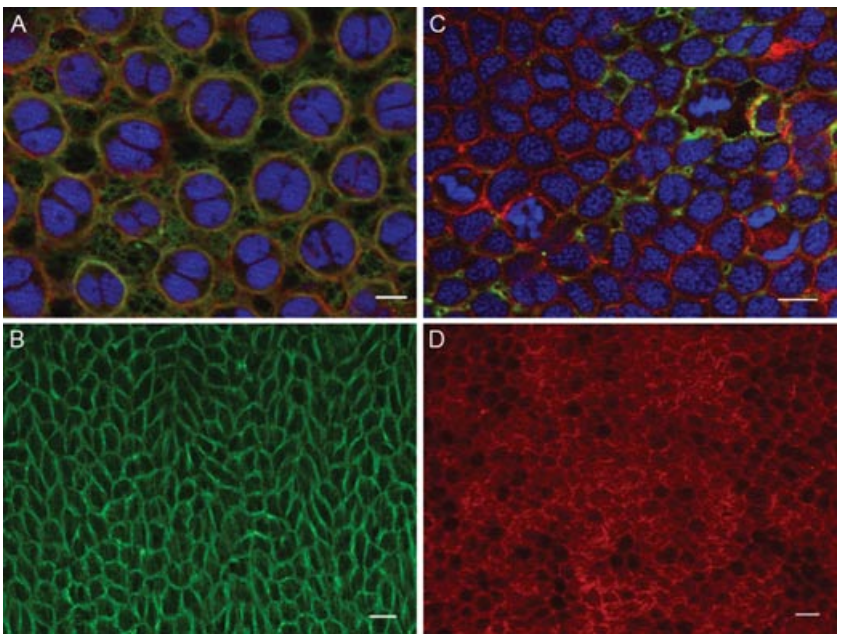

ectopic administration of JH decreased the expression of BgDcr1 mRNA, whereas the elimination of the JH source in allatectomised females elicited the reverse effect.

The expression of BgDcr1 in ovaries of dsBgDcr1-treated females was down-regulated 3 days after the treatment, with a concomitant depletion of the protein BgDcr1. Two days later, and quite unexpectedly, BgDcr1 mRNA levels had increased, suggesting the occurrence of efficient feedback mechanisms that allowed the observed expression recovery. However, dsBgDcr1-treated females arrested ovarian follicle development and never oviposit, which suggests that the observed mRNA rebound did not lead to increase BgDcr1 protein levels within the experimental time frame.

Depletion of BgDcr1 and, consequently, depletion of the miRNA affected both somatic and germinal cells, although the former was affected to a greater extent. It is therefore clear that changes in follicular epithelia were crucial to arrest oocyte development. The continuous cell division provokes that the follicular epithelium becomes compact, which does not allow that haemolymph circulating proteins, such as Vg and other storage molecules, reach the oocyte membrane.

In Dcr1 mutants of *D. melanogaster*, the female germline stem cells are not maintained and are lost from the niche in the germarium, thus suggesting that miRNAs modulate oogenesis (Jin and Xie, 2007). Likewise, follicular cells are perturbed by the absence of Dcr1, thus resulting in a delay in *Notch* activation and inactivation in these cells, produced via their ligand, *Delta*, which is an important miRNA target (Poulton et al., 2011). Conversely, treatment of the mosquito *A. aegypti*, with dsDcr1, depleted mRNA and miRNA expression in the fat body, although oocyte development in treated females was unaffected (Bryant et al., 2010).

Interestingly, when BgDcr1 levels are depleted by RNAi, miRNAs are generally down-regulated, as shown by the level measurements carried out on a selection of them. An exception to this is miR-305, which was up-regulated after dsBgDcr1 treatment, suggesting that this miRNA might interact directly with BgDcr1 mRNA expression. This kind of

regulatory mechanism is reminiscent of the feedback mechanism described in humans, where Dcr1 is targeted by let-7 in sites within the coding region (Forman et al., 2008). In *B. germanica*, target predictions using the RNAHybrid platform (Rehmsmeier et al., 2004) suggest that miR-305 has putative target sites in the BgDcr1 Open Reading Frame. Other miRNAs that could interact with BgDcr1 are miR-100, miR-125 and let-7, which are coded by the same polycistronic pri-miRNA in a number of species (Belles et al., 2012). However, in the absence of BgDcr1 (Figure 2), these three miRNA responded differentially, thus suggesting a different regulatory system for each one. The lack of a sequenced genome for *B. germanica* does not allow us to know if these three miRNAs are forming or not a polycistronic pri-miRNA, which could help to explain this differential expression.

Our work indicates that BgDcr1 is crucial for the correct development of oogenesis in *B. germanica*. The results also indicate that depletion of BgDcr1 leads to a general depletion of miRNA levels, as expected given the key role of Dcr1 in miRNA biogenesis. Thus, we hypothesise that the oogenesis deficiencies observed in the absence of BgDcr1 are ultimately due to the depleted levels of miRNAs. Thus, the next step should be to assess the above hypothesis by identifying which precise miRNAs might be involved in the regulation of oogenesis in our model, and work along this line is presently in progress in our laboratory.

Materials and Methods

Insect sampling

Specimens of *B. germanica* were obtained from a colony reared in the dark at 29 ± 1°C and 60–70% relative humidity. Newly ecdysed sixth female nymphs and adult females were selected and used at appropriate ages. In adult females, the length of the basal oocyte was used to stage the ovaries from 0 to 7 days. Newly emerged adult females were maintained with males during the whole of the first gonadotrophic cycle, and mating was confirmed at the end of experiments by assessing the presence of spermatozoa in the spermatheca. All dissections and tissues sampling were carried out on carbon dioxide-anaesthetised specimens. Tissues were frozen with liquid N_2, and preserved at −80°C until use.

RNA extraction and retrotranscription

Total RNA was isolated using miRNeasy® Mini Kit (Qiagen) from ovary pair obtained in chosen ages along the sixth nymphal instar and in adults during the first gonadotrophic cycle. An amount of 400 ng of each RNA extraction was reverse transcribed using NCode™ miRNA First-Strand complementary DNA (cDNA) Synthesis and quantitative real-time PCR (qRT-PCR) Kits (Invitrogen). All procedures were made following the manufacturer's protocols. RNA quantity and quality were estimated by spectrophotometric absorption at 260 nm in a Nanodrop Spectrophotometer ND-1000®.

Quantitative real-time PCR

qRT-PCR was used to study the expression of BgDcr1 (accession number CAX68236), the miRNA expression in ovary during the sixth nymphal instar and in the first gonadotrophic cycle, and to assess the effect of RNAi over mRNA levels. The U6 from *B. germanica* (accession number FR823379) was used as a reference. The efficiency of each primer used in qRT-PCR was first validated by constructing a standard curve through four serial dilutions of cDNA from ovaries. PCR reactions were made using the IQTM SYBR Green Supermix (BioRad) containing 200 nM of the specific primer and 200 nM of the Universal primer (Invitrogen) and were run in triplicate. Amplification reactions were carried out at 95°C for 2 min, and 40 cycles of 95°C for 15 s and 60°C for 30s, using MyIQ Single Color RT-PCR Detection System (BioRad). After the amplification phase, a dissociation curve was carried out to ensure that there was only one product. We followed a method based in threshold cycle (Ct) according to the Pfaffl mathematical model (Pfaffl, 2001), with no correction for efficiency. Results are given as copies of RNA per 1,000 copies of U6. PCR primers used in qRT-PCR expression studies were designed using the Primer Express 2.0 software (Applied Biosystems). All primer sequences used in the amplifications are described in Supplementary Table S1.

RNAi experiments

A dsRNA was prepared encompassing a 343 bp region placed between the RNaseI and RNaseII domains of *B. germanica* Dcr1 (BgDcr1-A). To assess the specificity of the effects observed, we repeated the experiments using an alternative dsRNA for BgDcr1, this time targeting a 469 bp region placed between the PAZ domain and the RNaseI domain, which we called dsBgDcr1-B (Gomez-Orte and Belles, 2009). As results were identical with both dsRNA, we refer along the paper to the results obtained with dsBgDcr1-A (from now dsBgDcr1). As control dsRNA (dsMock), we used a 307 bp sequence from *Autographa californica* nucleopolyhedrovirus (accession number K01149, from nucleotide 370 to 676). The preparation of the dsRNAs was carried out as described previously (Ciudad et al., 2006). Newly emerged sixth nymphal females or newly emerged adult females of *B. germanica* were injected into the abdomen with a dose of 3.5 μg/μl dsBgDcr1. Control specimens were injected with the same volume and dose of dsMock.

JH treatment and allatectomy experiments

Newly emerged adult females were topically treated with 20 μg of racemic JH III (Sigma) in 1 μl acetone. Controls received the same volume of acetone. Ovaries were explanted 24 h after JH treatment and mRNA levels of BgDcr1 measured. For allatectomy experiments, CA were removed in newly emerged adult females. Five days later, the complete explanation of the CA was assessed and the ovaries were dissected and stored at −80°C until processed.

Western blot

Newly emerged females treated with 3.5 μg of dsBgDcr1 or dsMock were dissected at the ages of 3 and 5days. Ovaries were homogenised in 50 μl of extraction buffer (150 mM NaCl; 1.0% Nonidet-P40 [Sigma]; 50 mM Tris, pH 8.0), including protease inhibitor cocktail (Roche), and stored at -20°C until use. Homogenates were analysed in 7.5% SDS/PAGE gels loading 0.1 ovary equivalents per lane. Gels were transferred to a nitrocellulose membrane (Protran, Schleicher and Schuell) and incubated with Dcr1 antibody (1/1,000; Abcam) for 1 h, and were then processed for SuperSignal West Femto (Pierce; Thermo Scientific), following the manufacturer's instructions.

Immunoflourescence and cell staining

For immunofluorescence and staining, ovaries from 3- and 5-day-old adult females were dissected in Ringer's solution and the individualised ovarioles with their sheaths removed were fixed during 20 min in 4% paraformaldehyde in PBS (0.2 mM, pH 6.8) at room temperature. After that, they were rinsed and permeabilised in PBS-T (PBS + 0.3% Triton X-100) for 3 × 10 min. Subsequently, the ovarioles were treated with proteinase K (50 μg/ml; Sigma) for 2 min and the solution was changed for glycine (2 mg/ml) for 2 min. After three rinses with PBS-T (10 min each), the ovarioles were fixed again during 20 min in 4% paraformaldehyde in PBS and rinsed with PBS-T for 3 × 10 min. Unspecific binding sites were blocked by 1 h incubation in PBT-BN (PBS-T with 0.5% BSA [Sigma] and supplemented with 5% nonimmune goat serum [Sigma]). The ovarioles were incubated overnight at 4°C in a monoclonal antibody raised against β-tubulin—anti-mouse IgG1 (E7 antibody, Developmental Studies Hybridoma Bank), diluted 1:50 in PBT-BN. And after three rinses (10 min each) in PBT-BN, they were transferred for 2 h to Alexa Fluor 488-conjugated goat–anti-mouse IgG (Invitrogen) diluted 1:400 in PBT-BN and rinsed with PBT-BN for 3 × 10 min. For F-actin visualisation, these ovarioles were incubated with Phalloidin–tetramethylrhodamine B isothiocyanate (TRITC; 5 μg/ml; Sigma) during 30 min and rinsed with PBT-BN for 3 × 10 min. Subsequently, the ovarioles were incubated with DAPI (1 μg/ml; Sigma) during 5 min, for nucleic acid visualisation, and rinsed again with PBT-BN for 3 × 10 min. The stained and rinsed ovarioles were mounted in Mowiol (Calbiochem). The whole-mount ovariole preparations were analysed by epifluorescence microscopy AxioImager.Z1 (ApoTome System, Zeiss). Diameter of follicular cells was measured in three oocytes from dsMock and dsBgDcr1 females ($n = 5$); measurements were carried out with the AxioVision 4.8 software (Zeiss).

Statistics

All results are indicated as mean ± SEM. Statistical analysis of gene expression values was carried out using one-way analysis of variance test to compare the expression of different miRNA in dsMock and dsBgDcr1 treatments ($P < 0.08$). Fold change expression was calculated using the relative expression software tool (REST), 2008 program (Pfaffl et al., 2002). This program calculates changes in gene expression between two groups, control and treated, using the corresponding distributions of Ct values as input. The program makes no assumptions about the distributions, evaluating the significance of the derived results by pairwise fixed reallocation randomisation test tool in REST.

Author contribution

E.D.T. and M.D.P. conceived and designed the experiments, performed them and analysed the data; M.D.P. obtained the funding and wrote the paper.

Funding

This work was supported by the Ministry of Science and Innovation, Spain (project BFU2008-00484 to M.D.P.). E.D.T. is recipient of a post-doctoral research grant (JAE-Doc 'Junta para la Ampliación de Estudios') financed by the 'Consejo Superior de Investigaciones Cientificas' and The European Social Fund.

Acknowledgements

The β-tubulin antibody developed by M.W. Klymkowsky was obtained from the Developmental Studies Hybridoma Bank developed under the auspices of the NICHD and maintained by the Department of Biology, The University of Iowa, Iowa City, IA 52242. We are grateful to Professor Xavier Belles for his helpful scientific discussions and critical comments on the manuscript.

Conflict of interest statement

The authors have declared no conflict of interest.

References

Abu-Hakima, R. and Davey, K.G. (1975) Two actions of juvenile hormone on the follicle cells of *Rhodnius prolixus* Stal. Can. J. Zool. **53**, 1187–1188

Belles, X., Cristino, A.S., Tanaka, E.D., Rubio, M. and Piulachs, M.D. (2012) MicroRNAs in insects. From molecular mechanisms to biological roles. In Insect Molecular Biology and Biochemistry. Gilbert L.I. (ed.). Elsevier, Amsterdam, 30–56

Bryant, B., Macdonald, W. and Raikhel, A.S. (2010) MicroRNA miR-275 is indispensable for blood digestion and egg development in the mosquito *Aedes aegypti*. Proc. Natl. Acad. Sci. U. S. A. **107**, 22391–22398

Bushati, N. and Cohen, S.M. (2007) MicroRNA functions. Annu. Rev. Cell Dev. Biol. **23**, 175–
205

Ciudad, L., Belles, X. and Piulachs, M.D. (2007) Structural and RNAi characterization of the German cockroach lipophorin receptor, and the evolutionary relationships of lipoprotein receptors. BMC Mol, Biol, **8**, 53

Ciudad, L., Piulachs, M.D. and Belles, X. (2006) Systemic RNAi of the cockroach vitellogenin receptor results in a phenotype similar to that of the *Drosophila* yolkless mutant. FEBS J. **273**, 325–335

Cristino, A.S., Tanaka, E.D., Rubio, M., Piulachs, M.-D. and Belles, X. (2011) Deep sequencing of organ- and stage-specific microRNAs in the evolutionarily basal insect *Blattella germanica* (L.) (Dictyoptera, Blattellidae). PLoS One **6**, e19350

Forman, J.J., Legesse-Miller, A. and Coller, H.A. (2008) A search for conserved sequences in coding regions reveals that the let-7 microRNA targets Dicer within its coding sequence. Proc. Natl. Acad. Sci. U. S. A. **105**, 14879–14884

Gomez-Orte, E. and Belles, X. (2009) MicroRNA-dependent metamorphosis in hemimetabolan insects. Proc. Natl. Acad. Sci. U. S. A. **106**, 21678–21682

Irles, P., Bellés, X. and Piulachs, M.D. (2009) Identifying genes involved in choriogenesis in insect panoistic ovaries by suppression subtractive hybridization. BMC Genomics **10**, 206.

Jagadeeswaran, G., Zheng, Y., Sumathipala, N., Jiang, H., Arrese, E.L., Soulages, J.L., Zhang, W. and Sunkar, R. (2010) Deep sequencing of small RNA libraries reveals dynamic regulation of conserved and novel microRNAs and microRNA-stars during silkworm development. BMC Genomics **11**, 52

Jaubert, S., Mereau, A., Antoniewski, C. and Tagu, D. (2007) MicroRNAs in *Drosophila*: the magic wand to enter the chamber of secrets? Biochimie. **89**, 1211–1220

Jin, Z. and Xie, T. (2007) Dcr-1 maintains *Drosophila* ovarian stem cells. Curr. Biol. **17**, 539–544

Legeai, F., Rizk, G., Walsh, T., Edwards, O., Gordon, K., Lavenier, D., Leterme, N., Mereau, A., Nicolas, J., Tagu, D. and Jaubert-Possamai, S. (2010) Bioinformatic prediction, deep sequencing of microRNAs and expression analysis during phenotypic plasticity in the pea aphid, Acyrthosiphon pisum. BMC Genomics **11**, 281

Luo, Q., Zhou, Q., Yu, X., Lin, H., Hu, S. and Yu, J. (2008) Genome-wide mapping of conserved microRNAs and their host transcripts in Tribolium castaneum. J. Genet. Genomics **35**, 349–355

Martin, D., Piulachs, M.D., Comas, D. and Belles, X. (1998) Isolation and sequence of a partial vitellogenin cDNA from the cockroach, *Blattella germanica* (L.) (Dictyoptera, Blattellidae), and characterization of the vitellogenin gene expression. Arch. Insect Biochem. Physiol. **38**, 137–146

Pfaffl, M.W. (2001) A new mathematical model for relative quantification in real-time RT-PCR. Nucleic Acids Res. **29**, e45

Pfaffl, M.W., Horgan, G.W. and Dempfle, L. (2002) Relative expression software tool (REST) for group-wise comparison and statistical analysis of relative expression results in real-time PCR. Nucleic Acids Res, **30**, e36

Poulton, J.S., Huang, Y.C., Smith, L., Sun, J., Leake, N., Schleede, J., Stevens, L.M. and Deng, W.M. (2011) The microRNA pathway regulates the temporal pattern of Notch signaling in *Drosophila* follicle cells. Development **138**, 1737–1745

Rehmsmeier, M., Steffen, P., Hochsmann, M. and Giegerich, R. (2004) Fast and effective prediction of microRNA/target duplexes. RNA **10**, 1507–1517

Shcherbata, H.R., Ward, E.J., Fischer, K.A., Yu, J.Y., Reynolds, S.H., Chen, C.H., Xu, P., Hay, B.A. and Ruohola-Baker, H. (2007) Stage-specific differences in the requirements for germline stem cell maintenance in the *Drosophila* ovary. Cell Stem Cell **1**, 698–709

Singh, J. and Nagaraju, J. (2008) *In silico* prediction and characterization of microRNAs from red flour beetle (Tribolium castaneum). Insect Mol. Biol. **17**, 427–436

Skalsky, R.L., Vanlandingham, D.L., Scholle, F., Higgs, S. and Cullen, B.R. (2010) Identification of microRNAs expressed in two mosquito vectors, Aedes albopictus and Culex quinquefasciatus. BMC Genomics **11**, 119

Stark, A., Kheradpour, P., Parts, L., Brennecke, J., Hodges, E., Hannon, G.J. and Kellis, M. (2007) Systematic discovery and characterization of fly microRNAs using 12 *Drosophila* genomes. Genome Res. **17**, 1865–1879

Treiblmayr, K., Pascual, N., Piulachs, M.D., Keller, T. and Belles, X. (2006) Juvenile hormone titer versus juvenile hormone synthesis in female nymphs and adults of the German cockroach, *Blattella germanica*. J. Insect Sci. **6**, 1–7

Weaver, D.B., Anzola, J.M., Evans, J.D., Reid, J.G., Reese, J.T., Childs, K.L., Zdobnov, E.M., Samanta, M.P., Miller, J. and Elsik, C.G. (2007) Computational and transcriptional evidence for microRNAs in the honey bee genome. Genome Biol. **8**, R97

Wei, Y., Chen, S., Yang, P., Ma, Z. and Kang, L. (2009) Characterization and comparative profiling of the small RNA transcriptomes in two phases of locust. Genome Biol. **10**, R6

Winter, F., Edaye, S., Huttenhofer, A. and Brunel, C. (2007) Anopheles gambiae miRNAs as actors of defence reaction against Plasmodium invasion. Nucleic Acids Res. **35**, 6953–6962

Received: 3 November 2011; Accepted: 26 March 2012; Accepted article online: 29 March 2012

